Modified embedded-atom method interatomic potentials for Ti and Zr

Young-Min Kim,[1] Byeong-Joo Lee,[1,*] and M. I. Baskes[2]
[1]*Department of Materials Science and Engineering, Pohang University of Science and Technology, Pohang 790-784, Republic of Korea*
[2]*Structure/Properties Relation Group, Los Alamos National Laboratory, Los Alamos, New Mexico 87545, USA*
(Received 3 January 2006; revised manuscript received 3 May 2006; published 7 July 2006)

Semiempirical interatomic potentials for hcp elements, Ti and Zr, have been developed based on the MEAM (modified embedded-atom method) formalism. The new potentials do not cause the stability problem previously reported in MEAM for hcp elements, and describe wide range of physical properties (bulk properties, point defect properties, planar defect properties, and thermal properties) of pure Ti and Zr, in good agreement with experimental information. The applicability of the potentials to atomistic approaches for investigation of various materials behavior (slip, irradiation, amorphous behavior, etc.) in Ti or Zr-based alloys is demonstrated by showing that the related material properties are correctly reproduced using the present potentials and that the potentials can be easily extended to multicomponent systems.

DOI: 10.1103/PhysRevB.74.014101 PACS number(s): 61.50.Lt, 62.20.Dc, 64.70.Dv, 64.70.Kb

I. INTRODUCTION

Ti and Zr have a wide range of technological application as high temperature materials, nuclear reactor materials, and amorphous materials. Depending on their own c/a ratios and compositions, hcp metal-based alloys are known to show different slip behavior which has not been clarified yet.[1,2] Since they do not easily absorb neutrons, zirconium alloys are widely used in nuclear reactors. Under irradiation, the Zr-based alloys are subjected to an anisotropic change of microstructure even in the absence of applied stress. This phenomenon, known as irradiation growth, is influenced by various physical-metallurgical factors (texture, grain size, dislocation density, and alloy content).[3,4] Also recently, various procedures have been developed to produce bulk amorphous alloys based on Ti and Zr, with scientific and industrial interest. Ti and Zr-based amorphous alloys show superb glass forming ability, excellent hardness, stiffness, and strength.[5] Because of the possibility of further improving mechanical properties by promoting the homogeneous precipitation of nanocrystallites within the amorphous matrix, a large number of experimental and theoretical investigations are being performed on the amorphous/nanocrystallites composites.[6,7]

All the above-mentioned materials properties of the Ti and Zr-based alloys, the slip behavior, irradiation behavior, and amorphous behavior can be best understood when the evolution of materials structure is examined on an atomistic level. The atomistic approach such as molecular dynamics (MD) or Monte Carlo (MC) simulation based on semiempirical interatomic potentials can be an effective way of analyzing atomic structures. The essence of semiempirical atomistic approaches is the reliability of the interatomic potential used. A reliable interatomic potential should reproduce various fundamental physical properties of relevant elements or alloys, such as elastic properties, structural properties, defect properties, surface properties, and thermal properties, etc.

The most widely used empirical many-body interatomic potential formalisms are the embedded-atom method (EAM) potential by Daw and Baskes[8] and the Finnis-Sinclair (F-S) potential by Finnis and Sinclair.[9] Both potentials have led to encouraging results in a number of atomistic studies for cubic transition and noble metals. But atomistic studies using empirical interatomic potentials have been less common for hcp elements than cubic elements because of the difficulty in obtaining suitable interatomic potentials for hcp elements.[10,11] The difficulty mainly comes from the large number of structural parameters which should be fitted to describe the lattice anisotropy; there are two lattice constants (not one as in cubic metals) and five elastic constants (not three) to consider. Despite these difficulties, because of the practical importance of hcp elements, a number of studies to develop empirical potentials for hcp elements have been steadily attempted.

The many-body interatomic potentials published for hcp elements are the EAM type, F-S type, and the RGL type proposed by Rosato-Guillopé-Legrand,[12] etc. The first many-body interatomic potential reported for hcp elements is the EAM type. The EAM potentials for hcp elements proposed by Johnson *et al.*[13–15] can fit the empirical energy-volume relationship of Rose *et al.*,[16] thereby ensuring reasonable properties away from equilibrium. In the first paper,[13] EAM potentials were derived for Mg, Ti, and Zr. These potentials reproduced five elastic constants, the stability of hcp structure, vacancy formation, and self-interstitial formation energy for Mg, Ti, and Zr, but all with nearly ideal c/a ratios. In the second paper[14] two model potentials which approximately match zirconium were described, one with c/a close to the ideal value and the other with $c/a=1.580$ which is below the experimental value of 1.593. These potentials showed the effect of the c/a ratio on lattice stability and point defect properties of hcp metals. In the third paper,[15] potentials were derived for Ti, but this model was constrained to an ideal c/a ratio (1.633). In a separate study for development of EAM potentials for hcp metals, Pasianot and Savino[17] have concluded that the elastic constants of several hcp pure metals cannot be correctly fitted within the EAM formalism. The present authors believe that the failure of the EAM in describing the physical properties of hcp elements comes from the lack of angular dependency in the EAM formalism. It should be noted here that a modified version of the EAM which is named the analytic modified embedded-

atom method (AMEAM) potential was recently proposed by Hu *et al.*[18] for hcp elements (Be, Co, Hf, Mg, Re, Ru, Sc, Ti, Y, and Zr). However, this potential can be used only for the cases where the z axis of coordinate system is parallel to the c axis of the hcp lattice.

The second interatomic potential reported for hcp elements is the F-S type. The F-S type potential proposed by Igarashi *et al.*[19] for eight elements, Be, Hf, Ti, Ru, Zr, Co, Mg, and Zn, were fitted to several physical parameters, including the c/a ratio. The pair repulsion term in this potential was too "hard" and the resultant formation energy values of self-interstitials were too large.[20] Ackland[20,21] developed F-S potentials for Ti and Zr by fitting to three elastic constants and one lattice constant. These potentials showed an improved description of atom-atom interactions inside the nearest-neighbor spacing and were employed successfully to investigate defects, surface and displacement-threshold properties, radiation damage, and twin boundary structures.[20,21] However, the F-S type potential appears to be less convenient for direct extension from pure elements to alloy systems.[22]

The third interatomic potential reported for hcp elements is the RGL type, initially proposed by Rosato *et al.* based on the tight-binding second moment approximation for fcc elements.[12] Willaime and Massobrio[23] developed a RGL type potential for Zr. The reliability of this potential was tested for both hcp and bcc-Zr with regard to point defect properties, thermal expansion, phonon properties, and mean-square displacements. Another RGL type potential for Ti and Zr has been also developed by Cleri and Rosato.[24]

In general, the RGL type potentials as well as all the above mentioned potentials have a difficulty in reproducing c/a ratio and other properties simultaneously. Furthermore, the above-mentioned potentials were rarely used to describe alloy systems including hcp elements.[22] Because most of industrial materials are not pure elements but multicomponent alloys, the application of semiempirical atomistic approaches would be highly enhanced if the potential formalism could be easily extended to describe multicomponent systems composed of various elements of difference types (equilibrium structures). In order to describe multicomponent systems easily, it is essential to be able to describe individual elements of different equilibrium structures using a common mathematical formalism.

The modified embedded-atom method (MEAM) formalism can describe a wide range of elements without changing the functional expression. From this point of view, the MEAM potential may be highly recommended for the description of alloy systems. The MEAM was created by Baskes, by modifying the[8] EAM so that the directionality of bonding is considered, and was applied to provide interatomic potentials of various fcc, bcc, diamond, and gaseous elements.[25] The MEAM has also been applied to develop interatomic potentials of hcp elements by Baskes and Johnson.[26] However, a critical problem on the structural stability was raised by Mae *et al.*,[27] who reported that out of the eighteen hcp elements described by the[26] MEAM only seven stay in the hcp structure after MD runs at finite temperatures while others result in a stable structure different from the hcp. Actually, a similar structural stability problem had been found also in the MEAM for bcc elements.[28] Therefore, the original MEAM was modified once again by Lee and Baskes[28,29] in order to solve the above mentioned stability problem in bcc elements. The new formalism considers up to second nearest neighbor interactions while the original MEAM considers only first nearest-neighbor interactions, and is named the second nearest neighbor (2NN) MEAM to distinguish it from the original MEAM. The original MEAM corresponds to a special case of the 2NN MEAM where the second and more distant nearest neighbor interactions are fully neglected. Later, similar stability problems were also found in the 1NN MEAM for some fcc elements.[30] Because those stability problems could be solved by applying the 2NN MEAM formalism,[30] it would be fruitful to apply it also to hcp elements and see whether the stability problems raised in hcp elements can be solved.

As a part of a long project to develop MEAM interatomic potentials of hcp elements, the 2NN MEAM formalism was first applied to two typical hcp elements, Ti and Zr. The purpose of the present work is to upgrade the MEAM interatomic potentials of Ti and Zr, solving the stability problem and describing fundamental physical properties of the elements better than any other empirical potential. In Sec. II the formalism of the (2NN) MEAM will be briefly described. In Sec. III the procedure for the determination of parameter values will be given. Comparisons between calculated and experimental physical properties and thermodynamic properties of Ti and Zr will be made in Sec. IV. The general performance of the present potentials will also be discussed in this section, and Sec. V is a conclusion.

II. FORMALISM

In the MEAM, the total energy of a system is approximated as

$$E = \sum_i \left[F_i(\bar{\rho}_i) + \frac{1}{2} \sum_{j(\neq i)} \phi_{ij}(R_{ij}) \right]. \tag{1}$$

F_i is the embedding function, $\bar{\rho}_i$ is the background electron density at site i, and ϕ_{ij} (R_{ij}) is the pair interaction between atoms i and j separated by a distance R_{ij}. For general calculations of energy, the functional forms for the two terms on the right hand side of Eq. (1), F_i and ϕ_{ij} should be given. The embedding function is given the following form[25]

$$F(\bar{\rho}) = AE_c \frac{\bar{\rho}}{\bar{\rho}^o} \ln \frac{\bar{\rho}}{\bar{\rho}^o}, \tag{2}$$

where A is an adjustable parameter, E_c is the cohesive energy, and $\bar{\rho}^o$ is the background electron density for a reference structure. The reference structure is a structure where individual atoms are on exact lattice points. Normally, the equilibrium structure is taken as the reference structure for elements. The background electron density $\bar{\rho}_i$ at a site is computed considering directionality in bonding, that is, by combining several partial electron density terms, $\rho_i^{(0)}$, $\rho_i^{(1)}$, $\rho_i^{(2)}$, $\rho_i^{(3)}$ for different angular contributions with weight factors $t^{(h)}$ $(h=1-3)$. Each partial electron density term has the following form[25]

$$(\rho_i^{(0)})^2 = \left[\sum_{j\neq i} \rho_j^{a(0)}(R_{ij})\right]^2, \tag{3a}$$

$$(\rho_i^{(1)})^2 = \sum_{\alpha}\left[\sum_{j\neq i} \frac{R_{ij}^{\alpha}}{R_{ij}}\rho_j^{a(1)}(R_{ij})\right]^2, \tag{3b}$$

$$(\rho_i^{(2)})^2 = \sum_{\alpha,\beta}\left[\sum_{j\neq i} \frac{R_{ij}^{\alpha}R_{ij}^{\beta}}{R_{ij}^2}\rho_j^{a(2)}(R_{ij})\right]^2 - \frac{1}{3}\left[\sum_{j\neq i}\rho_j^{a(2)}(R_{ij})\right]^2, \tag{3c}$$

$$(\rho_i^{(3)})^2 = \sum_{\alpha,\beta,\gamma}\left[\sum_{j\neq i} \frac{R_{ij}^{\alpha}R_{ij}^{\beta}R_{ij}^{\gamma}}{R_{ij}^3}\rho_j^{a(3)}(R_{ij})\right]^2 - \frac{3}{5}\sum_{\alpha}\left[\sum_{j\neq i} \frac{R_{ij}^{\alpha}}{R_{ij}}\rho_j^{a(3)}(R_{ij})\right]^2. \tag{3d}$$

Here, $\rho_j^{a(h)}$ represent atomic electron densities from j atom at a distance R_{ij} from site i. R_{ij}^{α} is the α component of the distance vector between atoms j and i ($\alpha=x,y,z$). The partial electron densities are equivalent to an expansion of density in Legendre polynomials. The way of combining the partial electron densities to give the total background electron density is not unique, and several expressions have been proposed.[31] Among them, the following form that can be widely used without numerical error is taken in the present work.

$$\bar{\rho}_i = \rho_i^{(0)} G(\Gamma), \tag{4}$$

where

$$G(\Gamma) = \frac{2}{1+e^{-\Gamma}}, \tag{5}$$

and

$$\Gamma = \sum_{h=1}^{3} t_i^{(h)}\left[\frac{\rho_i^{(h)}}{\rho_i^{(0)}}\right]^2, \tag{6}$$

$t_i^{(h)}$ are adjustable parameters. The atomic electron density is given as

$$\rho_j^{a(h)}(R) = e^{-\beta^{(h)}(R/r_e-1)}, \tag{7}$$

where $\beta^{(h)}$, the decay lengths are adjustable parameters and r_e is the nearest-neighbor distance in the equilibrium reference structure.

As shown above, a specific form is given to the embedding function F_i, but not to the pair interaction ϕ_{ij}. Instead, the total energy per atom for the equilibrium reference structure is estimated from the zero-temperature universal equation of state by Rose *et al.*[16] as a function of nearest-neighbor distance R.

$$E^u(R) = -E_c(1+a^*+da^{*3})e^{-a^*}, \tag{8}$$

where d is an adjustable parameter, and

$$a^* = \alpha(R/r_e - 1), \tag{9}$$

and

$$\alpha = \left(\frac{9B\Omega}{E_c}\right)^{1/2}. \tag{10}$$

$E^u(R)$ is the universal function for a uniform expansion or contraction in the reference structure, B is the bulk modulus, and Ω is the equilibrium atomic volume.

Once the total energy per atom and embedding function are computed for a reference structure, the values of the pair interaction can be numerically obtained using Eq. (1), as a function of nearest-neighbor distance. Details of this procedure for the 1NN and 2NN MEAM are given in the Appendix.

In the original MEAM,[25] only first nearest-neighbor interactions are considered, as mentioned already. The neglect of the second and more distant nearest-neighbor interactions is made effective by the use of a strong many-body screening function.[31] The consideration of the second nearest-neighbor interactions in the modified formalism (the[28–30] 2NN MEAM) is affected by adjusting screening parameters, $C_{\min}$ and $C_{\max}$, so that the many-body screening becomes less severe. In the MEAM, the many-body screening function between atoms i and j, S_{ij}, is defined as the product of the screening factors, S_{ikj}, due to all other neighbor atoms k

$$S_{ij} = \prod_{k\neq i,j} S_{ikj}. \tag{11}$$

The screening factor S_{ikj} is computed using a simple geometric construction. Imagine an ellipse on an x, y plane, passing through atoms, i, k, and j with the x axis of the ellipse determined by atoms i and j. The equation of the ellipse is given by

$$x^2 + \frac{1}{C}y^2 = \left(\frac{1}{2}R_{ij}\right)^2. \tag{12}$$

For each k atom, the value of parameter C can be computed from relative distances among the three atoms, i, j and k, as follows:

$$C = \frac{2(X_{ik}+X_{kj}) - (X_{ik}-X_{kj})^2 - 1}{1-(X_{ik}-X_{kj})^2}, \tag{13}$$

where $X_{ik}=(R_{ij}/R_{ij})^2$ and $X_{kj}=(R_{kj}/R_{ij})^2$. The screening factor, S_{ikj} is defined as a function of C as follows:

$$S_{ikj} = f_c\left[\frac{C-C_{\min}}{C_{\max}-C_{\min}}\right], \tag{14}$$

where $C_{\min}$ and $C_{\max}$ are the limiting values of C determining the extent of screening and the smooth cutoff function is

$$f_c(x) = 1 \quad x \geqslant 1,$$

$$[1-(1-x)^4]^2 \quad 0 < x < 1,$$

$$0 \quad x \leqslant 0. \tag{15}$$

The basic idea for the screening is that: First define two limiting values, $C_{\max}$ and $C_{\min}$ ($C_{\max} > C_{\min}$). Then, if the atom k is outside of the ellipse defined by $C_{\max}$, it is assumed that the atom k does not have any effect on the interaction

TABLE I. MEAM potential parameters for Ti and Zr. The units of the cohesive energy E_c, the equilibrium nearest neighbor distance r_e and the bulk modulus B are eV, Å and 10^{12} dyne/cm^2, respectively.

	E_c	r_e	B	A	$\beta^{(0)}$	$\beta^{(1)}$	$\beta^{(2)}$	$\beta^{(3)}$	$t^{(1)}$	$t^{(2)}$	$t^{(3)}$	$C_{\min}$	$C_{\max}$	d
Ti	4.87	2.92	1.10	0.66	2.70	1.00	3.00	1.00	6.80	−2.00	−12.00	1.00	1.44	0.00
Zr	6.36	3.20	0.97	0.68	2.45	1.00	3.00	2.00	6.30	−3.30	−10.00	1.00	1.44	0.00

between atoms i and j. If the atom k is inside of the ellipse defined by $C_{\min}$ it is assumed that the atom k completely screens the i-j interaction, and between $C_{\max}$ and $C_{\min}$ the screening changes gradually. In the numerical procedure the electron density and pair potential are multiplied by the screening function S_{ij}. Therefore, $S_{ij}=1$ and $S_{ij}=0$ mean that the interaction between atoms i and j is unscreened and completely screened, respectively. In addition to the many-body screening function, a radial cutoff function which is given by $f_c[(r_c-r)/\Delta r]$ where r_c is the cutoff distance and Δr (0.1 Å) is the cutoff region, is also applied to the atomic electron density and pair potential.[31] The radial cutoff distance is chosen so that it does not have any effect on the calculation results due to the many-body screening. This is only for the computational convenience, that is, to save computation time in developing neighbor lists.

III. DETERMINATION OF POTENTIAL PARAMETERS

The 2NN MEAM formalism for elements was applied to evaluate the MEAM parameters for the hcp elements Ti and Zr. The parameters were determined by fitting to physical properties of Ti and Zr, as will be described. The parameters finally determined for Ti and Zr are listed Table I. Here, the reference structure is hcp. In this section, the procedure for the determination of these parameter values will be presented.

The 2NN MEAM formalism[29,30] gives fourteen independent model parameters for pure elements: four (E_c, r_e, B, d) for the universal equation of state, seven ($\beta^{(0)}$, $\beta^{(1)}$, $\beta^{(2)}$, $\beta^{(3)}$, $t^{(1)}$, $t^{(2)}$, $t^{(3)}$) for the electron density, one (A) for the embedding function, and two ($C_{\min}$, $C_{\max}$) for the many-body screening. Out of the fourteen parameters, E_c, r_e, and B are cohesive energy, nearest neighbor distance and bulk modulus of the reference structure, respectively. When a real structure is selected as the reference structure, these parameters become material properties, not model parameters, and the values can be obtained experimentally. In the present study, hcp structure was selected as the reference structure of MEAM Ti and Zr, and the values of the above three parameters were obtained from experimental information on hcp Ti and Zr.

The adjustable parameters whose values should be actually determined by fitting to physical properties totaled eleven, (A, $\beta^{(0)}$, $\beta^{(1)}$, $\beta^{(2)}$, $\beta^{(3)}$, $t^{(1)}$, $t^{(2)}$, $t^{(3)}$, $C_{\min}$, $C_{\max}$, d). For the determination of the adjustable parameter values, a similar procedure to the previous ones for[29] bcc and[30] fcc elements was used. In the present work for Ti and Zr, elastic constants, structural energy differences, surface energy, stacking fault energy, and vacancy formation energy were used for the determination of model parameter values. Also, special attention was paid to the stability of hcp structure at finite temperatures.

The procedure for determining the model parameter values begins with determining the value of d. This value could be determined separately from the other parameters and could be only determined by fitting the $(\partial B/\partial P)$ value. It had been decided in the previous study on bcc elements[29] to give either 0 or 0.05 to d according to the $(\partial B/\partial P)$ value from experiments or first-principles calculations. This was because the experimental information on $(\partial B/\partial P)$ was not always available and the accuracy of first-principles calculations was not very good to be used for the determination of the d value as a material constant. The $(\partial B/\partial P)$ value from first-principles calculations for Ti and Zr were 4.65 and 4.43,[16] respectively. According to the present calculation, these values were 4.14 and 3.97 with $d=0$, and were 4.62 and 4.41 with $d=0.05$. This implies that 0.05 should be given to the d parameter when considering the first-principles calculations. However, it was also found that the first-principles calculations overestimate the $(\partial B/\partial P)$ values for other elements (Nb, Ta, Mo, W) close to Ti and Zr on the Periodic Table by more than 15% compared to experimental values. For example, the first principles values were 4.72 and 4.77 for Mo and W while corresponding experimental values were 4.1 and 3.8, respectively.[16] Therefore, a final decision was made in the present study to give the value zero to the d parameter for Ti and Zr.

After the d value is determined, all the other model parameters (A, $\beta^{(0)}$, $\beta^{(1)}$, $\beta^{(2)}$, $\beta^{(3)}$, $t^{(1)}$, $t^{(2)}$, $t^{(3)}$, $C_{\min}$, $C_{\max}$) are determined by fitting to physical properties of Ti and Zr. In the previous studies for bcc and fcc elements,[29,30] a fixed value of 2.80 which was the same as in the original[25] MEAM was given to the $C_{\max}$ parameter. In the present study, the same value was initially given to $C_{\max}$ and the parameter optimization was started by giving a specific value to $C_{\min}$. Generally, the effect of each parameter on individual properties is complicated, and it is impossible to relate one property only to one parameter. However, the effects of some parameters are certainly confined to only few properties, and the evaluation of parameters can be done systematically. Table II shows which parameters have effects on which properties. A and $\beta^{(0)}$ values are given considering elastic constants and also roughly considering energy differences among hcp, bcc, and fcc structures. Then, the $\beta^{(1)}$, $\beta^{(2)}$, $\beta^{(3)}$ parameter values are adjusted so that elastic constants are reproduced more accurately. Finally, the $t^{(1)}$, $t^{(2)}$, $t^{(3)}$ parameter values are determined fitting to surface energies, vacancy formation energy, structural energy differences, and stacking faults energy. All target properties are not completely reproduced by this procedure. The above procedure is repeated changing $C_{\min}$ value until most of the target properties are correctly

TABLE II. Effect of parameters on individual properties of Ti and Zr. The plus sign links individual parameters and relevant properties that can be used for determination of the parameter value.

	A	$\beta^{(0)}$	$\beta^{(1)}$	$\beta^{(2)}$	$\beta^{(3)}$	$t^{(1)}$	$t^{(2)}$	$t^{(3)}$
C_{11}	+	+	+					+
C_{12}	+	+	+	+	+			+
C_{66}	+	+	+	+	+			+
C_{44}	+	+	+	+	+			+
C_{33}	+	+	+	+	+			+
C_{13}	+	+	+			+	+	+
$E_{(\text{basal})}$	+	+	+			+	+	+
$E_{(\text{prism})}$	+	+	+			+	+	+
E^f_V	+		+			+	+	+
E^f_I	+	+		+	+	+	+	+
E_{sf} (I_2)	+							+
$\Delta E_{hcp\rightarrow bcc}$	+	+						+
$\Delta E_{hcp\rightarrow fcc}$	+	+						+

reproduced. The thermal expansion coefficient is also considered when adjusting the $C_{\min}$ value. When all target property values are satisfactorily reproduced, a final check is made on the stability of the hcp structure at finite temperatures. This is because the stability problem of the hcp structure has been a big issue, and solving it was one of the main purposes of the present work. Even in the present parametrization, with the initial value 2.80 of $C_{\max}$, a slightly modified structure which is certainly different from hcp was indeed generated after MD runs at finite temperatures. The formation of this structure could be avoided by lowering the $C_{\max}$ parameter value. Therefore, the above procedure was repeated again changing $C_{\max}$ value until a parameter set that does not cause the stability problem and describes all the target properties satisfactorily is obtained. Table I shows the resultant MEAM parameters.

IV. RESULTS AND DISCUSSION

The potentials determined by the above procedure will now be used to compute various physical properties of Ti and Zr in order to evaluate their reliability. The 2NN MEAM formalism includes up to second nearest neighbor interactions. Therefore, the radial cutoff distance during atomistic calculations should be at least larger than the second nearest neighbor distance in the structures under consideration. The recommended value is the mean value between the second and third nearest-neighbor distances. All calculations presented here are those performed with radial cutoff distances 4.80 Å and 5.20 Å for Ti and Zr, respectively.

The calculations were performed for bulk properties (lattice constants, elastic constants, structural energy differences), point defect properties (vacancy, divacancy and interstitial formation energy, activation energy of vacancy diffusion), planar defect properties (stacking faults energy, surface energy) and thermal properties (thermal expansion coefficients, specific heat, melting point, enthalpy of melting). All calculations except thermal properties are performed at 0 K, allowing full relaxations of individual atoms. Comparisons between the present calculations and experimental property values are presented in Table III and Table IV for Ti and Zr, respectively. Here, properties marked with a " *" are those used for fitting in the present work. Calculated values using other empirical potentials are also compared in Tables III and IV.

Concerning the cohesive energy E_c, it is shown that the calculated values are slightly lower than the given experimental values.[26] This is because of the c/a relaxation of lattice parameters from the ideal value, 1.633.[32] (For the reference structure, the cohesive energy could be adjusted so that an exact value is obtained after the relaxation, but this was thought marginal.) Among the other target properties the elastic constants[33] were given the highest weight during the fitting procedure, because it was thought that the accuracy of experimental measurements of elastic constants is higher than those of other properties. The calculated elastic constants are all relaxed values as already mentioned. The relaxation contributions [as defined as (C_unrelaxed—C_relaxed)/C_unrelaxed] are 1.8%, −4.1%, and 6.6% for C_{11}, C_{12} and C_{66} of Ti, and are 1.3%, −2.8%, and 4.6% for the same quantities of Zr, respectively. The relaxation contributions for other elastic constants are negligible. The experimental data being compared with computed structural energy differences, $\Delta E_{hcp\rightarrow bcc}$ and $\Delta E_{hcp\rightarrow fcc}$, are thermodynamically assessed values using the CALPHAD method.[34] It is shown that the present potentials can describe bulk properties of Ti and Zr as satisfactorily as any other empirical potential. It was also confirmed during the present study that the hcp is the most stable structure for Ti and Zr when compared with other structures such as simple cubic, diamond, A15 (Cr_3Si type) etc. as well as the fcc and bcc.

In the case of point defect properties, the vacancy formation energy and the activation energy of vacancy diffusion are experimentally available for Ti and Zr. For Zr, experimental information on the vacancy migration energy is also available. In Tables III and IV, two different calculated values are given for the vacancy migration energy, activation energy of vacancy diffusion, and the divacancy formation energy, one for in-basal plane migration or formation (designated as "In") and the other for out-of-basal plane migration or formation (designated as "Out"). The present potentials reproduce both of the vacancy formation energy and the activation energy of vacancy diffusion in good agreement with experimental data,[35–39] though the agreement in the vacancy migration energy in Zr is worse. In Tables III and IV, several self-interstitial formation energies for various self-interstitial sites are also presented. The self-interstitial sites are shown in Fig. 1. An O site is centered in an octahedron, a T site in a tetrahedron, a C site (crowdion) is midway between two out-of plane nearest neighbor atoms, and an S site is a split configuration normal to the basal plane. Similarly, for interstitials in the basal plane, a B_O site is below an O site, a B_T site is below a T site, a B_C site is midway between two in-plane nearest neighbors. Here, "unstable" means the given self-interstitial atom moves to another self-interstitial site after relaxation.

For surface energies, only average values for polycrystalline solids are available in the literature, while calculations

TABLE III. Calculated physical properties of Ti using the present MEAM potential, in comparison with experimental data. Values listed are the cohesive energy E_c (eV), the lattice parameter a and c (Å), the elastic constants B, C_{11}, C_{12}, C_{66}, C_{44}, C_{33}, C_{13} (10^{12} dyne/cm^2), the structural energy differences ΔE (eV/atom), the relaxed vacancy formation energy E^f_V, vacancy migration energy, activation energy of vacancy diffusion, divacancy formation energy (eV), the self-interstitial formation energy E^f_I (eV), the basal plane, prism plane and pyramidal plane surface energy (erg/cm^2), the stacking fault energy E_{sf} (erg/cm^2), thermal expansion coefficient ε (10^{-6}/K), specific heat C_p (J/mol·K), melting point (K), enthalpy of melting ΔH_m (kJ/mol), and volume change on melting $\Delta V_m/V_{solid}$ (%). Properties marked with a " *" are those used for fitting in the present work.

Ti		EAM Ref. 13	EAM Ref. 15		F-S Ref. 20	RGL Ref. 24		AMEAM Ref. 18	MEAM [Baskes] Ref. 26	MEAM [Present Work]	Exp.
*E_c			−4.855	−4.855		−4.853		−4.8541	−4.8771	−4.873	−4.870[a]
*Lattice parameter, a			2.922	2.922	—	2.492	—	—	2.951	2.945	2.951[b]
*Lattice parameter, c		—	4.772	4.772	—	3.961	—	—	4.675	4.687	4.679[b]
*c/a ratio (relative to ideal)		0.990	1.000	1.000	0.975	0.972	1.001	1.000	0.970	0.974	0.971[b]
*B		—	1.099	1.099	—	1.066	1.105	—	1.051	1.097	1.097[c]
*C_{11}		1.835	1.842	1.954	1.800	1.473	1.796	—	1.778	1.701	1.761[c]
*C_{12}		0.780	0.785	0.737	0.873	0.785	0.747	—	0.778	0.804	0.869[c]
*C_{66}		0.443	0.529	0.609	0.464	0.344	0.525	—	0.499	0.448	0.446[c]
*C_{44}		0.409	0.417	0.481	0.514	0.305	0.375	—	0.468	0.421	0.508[c]
*C_{33}		1.992	1.938	2.067	2.170	1.980	2.178	—	1.756	1.871	1.905[c]
*C_{13}		0.670	0.673	0.609	0.766	0.764	0.596	—	0.647	0.748	0.683[c]
*$\Delta E_{hcp\to bcc}$		0.020	—	—	—	—	—	0.0143	0.075	0.024	0.070[d]
*$\Delta E_{hcp\to fcc}$		0.005	—	—	—	—	—	0.0094	0.033	0.048	0.060[d]
*E^f_v		1.55	1.49	1.48	1.43	—	—	1.49	1.78	1.79	>1.50[e]
Vacancy migration energy	In	—	0.67	0.82	—	—	—	0.61	—	1.09	—
	out	—	0.82	0.96	—	—	—	0.56	—	0.87	—
Activation energy of vacancy diffusion	In	—	2.16	2.30	—	—	—	2.10	—	2.88	3.14[f]
	out	—	2.31	2.44	—	—	—	2.05	—	2.66	
Divacancy formation energy	In	—	2.76	2.73	—	—	—	2.79	3.69	3.87	—
	out	—	2.76	2.73	—	—	—	2.78	3.67	3.90	—
E^f_I	C	3.76	—	3.82	3.07±0.2	—	—	2.92	—	3.90	—
	O	3.86	—	3.45	3.07±0.2	—	—	2.92	—	4.53	—
	S	4.04	—	4.05	3.07±0.2	—	—	3.15	—	4.32	—
	T	unstable	—	3.39	3.07±0.2	—	—	2.92	—	unstable	—
	B_O	3.79	—	3.33	3.07±0.2	—	—	3.07	—	3.73	—
	B_T	—	—	3.45	3.07±0.2	—	—	2.96	—	4.37	—
	B_C	unstable	—	3.70	3.07	—	—	2.96	—	3.78	—
*E_{surf}	basal$_{(0001)}$	—	—	—	993	—	—	1033	1962	2144	2100[e]
	prism$_{(1\bar{1}00)}$	—	—	—	1061	—	—	1023	1673	2145	1920[g]
	prism$_{(11\bar{2}0)}$	—	—	—	1187	—	—			2352	
	pyramidal$_{(1\bar{1}01)}$	—	—	—	1039	—	—	—	—	2444	
	pyramidal$_{(1\bar{1}02)}$	—	—	—	1194	—	—	—	—	2627	
*$E_{sf}(I_2)$		—	—	—	64	—	—	47	144	213	290[h] 300[i]
*ε(0–100 °C)		—	—	—	—	—	—	—	—	10.2	8.9[j]
C_p(0–100 °C)		—	—	—	—	—	—	—	—	25.8	25.3[j]

TABLE III. (*Continued.*)

Ti	EAM Ref. 13	EAM Ref. 15	F-S Ref. 20	RGL Ref. 24	AMEAM Ref. 18	MEAM [Baskes] Ref. 26	MEAM [Present Work]	Exp.
Melting point	—	— —	—	—	— —	—	1706	1941[d] (1737[d,k])
ΔH_m	—	— —	—	—	— —	—	14.50	14.15[d] (13.02[d,k])
$\Delta V_m/V_{solid}$	—	— —	—	—	— —	—	4.08	—

[a]Reference 26.
[b]Reference 32.
[c]Reference 33.
[d]Reference 34.
[e]Reference 35.
[f]Reference 36.
[g]Reference 42.
[h]Reference 43.
[i]Reference 44.
[j]Reference 45.
[k]for metastable melting of hcp Ti (calculated).

can be performed for several planes such as basal plane, prism planes, and pyramidal planes. All the experimental surface energy values are extrapolated values from high-temperature experimental data through some modeling approaches on the temperature dependence of surface energy.[35,42] On the basal plane, there are two intrinsic and one extrinsic stacking faults, where I_1 corresponds to *ABABCBCB*, I_2 to *ABABCACA*, and E to *ABABCABAB*. I_2 is the most important stacking fault in connection with plastic deformations (dislocation splitting into Shockley partials). Therefore, the I_2 stacking fault energy has been calculated in most empirical potential studies, and a comparison with experimental data[43,44] is made in Tables III and IV. It should be noticed here that the present potentials show the best agreement with experimental data for the stacking fault energy as well as the surface energy.

The next properties calculated using the present MEAM potential are the thermal properties such as thermal expansion coefficient, specific heat, melting point, enthalpy of melting, and volume change on melting. The results are compared with available experimental data[34,45] in Tables III and IV. The thermal expansion coefficients and specific heats were calculated in a temperature range of $0 \sim 100\ ^\circ\mathrm{C}$. The melting points were calculated using an interface velocity method. The enthalpies of melting and volume changes are those calculated at the calculated melting points of individual elements. Agreement with experimental data is acceptable except the volume change during melting where experimental data is not available. However, it should be mentioned here that the present MEAM potentials do not yield the experimentally observed hcp→bcc phase transformations at high temperature (1155 and 1139 K for Ti and Zr, respectively). Therefore, the calculated melting points, enthalpy and volume changes on melting listed in Tables III and IV are actually for the metastable melting of hcp Ti or Zr, while experimental data are for melting of bcc Ti or Zr. Values given in parentheses are for metastable melting of hcp Ti or Zr, obtained by a thermodynamic calculation using assessed thermodynamic parameters.[34]

The stability and physical properties of bcc Ti and Zr were further investigated. Though the high temperature hcp →bcc transformations are not reproduced correctly by the present potentials, the bcc structures are at least metastable yielding comparable melting points with hcp structures and allow calculation of physical properties. The lattice parameter, bulk modulus and elastic constants are in good agreement with available experimental data[50] as shown in Table V. Because the physical properties of bcc structures are reasonably described and the atomic structures are kept during MD runs up to their melting points, it would be possible to examine hcp/bcc interfacial structures and also mechanical properties of bcc structures at finite temperatures reliably using the present potentials. It is believed that the present potential can also be extended confidently into alloy systems where the bcc solid solution has a wide solubility range.

Finally it should be reminded that a correlation has been observed between the change in c/a and that in the slip behavior of hcp-metal based alloys. Therefore, it is important to know if the present potentials can reproduce the temperature dependence of the c/a ratios of Ti and Zr. For this, the lattice expansions in the a and c directions were calculated at various temperatures and were compared with experimental data,[46–49] as shown in Figs. 2 and 3. Here, the lattice expansion represents fractional change (%) relative to lattice parameters at 293 K. The present calculations show that the thermal expansion in the c direction is higher than that in the a direction for both Ti and Zr, in good agreement with experimental data, though somewhat larger values than experimental data are obtained for Zr.

It has been shown that the present MEAM potentials can reproduce a wide range of material properties (bulk, defect, and thermal properties) of Ti and Zr in good agreement with experimental information. The MEAM parameter sets (Table I) also show that the resultant potentials for Ti and Zr correspond to the 1NN MEAM (In the 2NN MEAM, second nearest-neighbor interactions are not considered for the hcp reference structure when the $C_{\min}$ value is larger than 1.0). This means that these elements could be described using the original 1NN MEAM formalism even though the starting formalism for the present parametrization was the more general 2NN MEAM. One strong point of the present potential is that the mathematical formalism is exactly the same as

TABLE IV. Calculated physical properties of Zr using the present MEAM potential, in comparison with experimental data. Values listed are the cohesive energy E_c (eV), the lattice parameter a and c (Å), the elastic constants B, C_{11}, C_{12}, C_{66}, C_{44}, C_{33}, C_{13} (10^{12} dyne/cm^2), the structural energy differences ΔE (eV/atom), the relaxed vacancy formation energy $E^f{}_V$, vacancy migration energy, activation energy of vacancy diffusion, divacancy formation energy (eV), the self-interstitial formation energy $E^f{}_I$ (eV), the basal plane, prism plane and pyramidal plane surface energy (erg/cm^2), the stacking fault energy E_{sf} (erg/cm^2), thermal expansion coefficient ε (10^{-6}/K), specific heat C_p (J/mol·K), melting point (K), enthalpy of melting ΔH_m (kJ/mol), and volume change on melting $\Delta V_m/V_{solid}$ (%). Properties marked with a "*" are those used for fitting in the present work.

Zr		EAM Ref. 13	EAM Ref. 14		F-S Ref. 21	RGL Refs. 23 and 24				AMEAM Ref. 18	MEAM [Baskes] Ref. 26	MEAM [Present Work]	Exp.
*E_c		—	−6.25	−6.25	−6.25	−6.17	−6.17	−6.167	−6.167	−6.2529	−6.3705	−6.364	−6.36[a]
*Lattice parameter, a		—	—	—	3.249	3.2196	3.202	3.232	—	—	3.237	3.231	3.231[b]
*Lattice parameter, c		—	—	—	5.189	5.247	5.218	5.147	—	—	5.153	5.125	5.148[b]
*c/a ratio (relative to ideal)		0.994	0.968	0.995	0.978	0.998	0.998	0.975	1.005	—	0.975	0.971	0.976[b]
*B		—	—	—	—	0.970	1.010	0.936	0.958	—	0.952	0.968	0.967[c]
*C_{11}		1.589	1.479	1.644	1.50	1.540	1.620	1.301	1.644	—	1.520	1.515	1.554[c]
*C_{12}		0.703	0.663	0.722	0.85	0.700	0.770	0.690	0.621	—	0.740	0.718	0.672[c]
*C_{66}		0.443	0.408	0.461	0.325	0.420	0.425	0.306	0.512	—	0.386	0.399	0.441[c]
*C_{44}		0.344	0.392	0.336	0.36	0.340	0.300	0.261	0.368	—	0.332	0.341	0.363[c]
*C_{33}		1.730	1.827	1.618	1.75	—	—	1.744	1.898	—	1.533	1.606	1.725[c]
*C_{13}		0.610	0.662	0.602	0.67	0.650	0.650	0.657	0.473	—	0.632	0.661	0.646[c]
*$\Delta E_{hcp\rightarrow bcc}$		0.040	0.0011	0.0427	—	—	0.03	—	—	0.0179	0.061	0.019	0.076[d]
*$\Delta E_{hcp\rightarrow fcc}$		0.003	0.0149	0.001	—	—	—	—	—	0.0049	0.017	0.055	0.076[d]
*E^f_v		1.36	1.86	1.63	1.786	—	2.07	—	—	1.70	1.93	2.09	>1.70[e]
Vacancy migration energy	In	—	0.775	1.00	—	—	0.88	—	—	0.72	—	1.14	0.54–0.62[f]
	out	—	0.785	1.06	—	—		—	—	0.67	—	0.89	0.6–0.7[g]
Activation energy of vacancy diffusion	In	—	2.635	2.63	—	—	2.95	—	—	2.42	—	3.23	3.17[h]
	out	—	2.645	2.69	—	—		—	—	2.37	—	2.98	
Divacancy formation energy	In	—	3.472	3.03	3.372	—	—	—	—	3.18	4.39	4.55	—
	out	—	3.484	3.032	3.379	—	—	—	—	3.18	4.38	4.59	—
E^f_v	C	4.52	3.66	4.49	3.979	—	4.27	—	—	3.60	—	4.04	3.07[i], 3.08[j]
	O	4.62	3.72	4.59	unstable	—	4.48	—	—	3.57	—	5.15	2.79[i], 2.84[j]
	S	4.92	3.91	4.83	4.319	—	unstable	—	—	3.57	—	4.62	2.80[i], 3.01[j]
	T	unstable	unstable	unstable	unstable	—	unstable	—	—	3.57	—	unstable	unstable[j]
	B_O	4.73	3.47	4.63	3.970	—	4.32	—	—	3.58	—	4.08	2.78[i], 2.88[j]
	B_T	—	—	—	unstable	—	unstable	—	—	3.51	—	5.02	4.03[j]
	B_C	unstable	—	—	3.756	—	unstable	—	—	3.52	—	4.14	2.95[j]

TABLE IV. (*Continued.*)

Zr		EAM Ref. 13	EAM Ref. 14	F-S Ref. 21	RGL Refs. 23 and 24	AMEAM Ref. 18	MEAM [Baskes] Ref. 26	MEAM [Present Work]	Exp.
	basal$_{(0001)}$	—	—	1022	—	988	2302	2156	2000[e]
	prism$_{(1\bar{1}00)}$	—	—	1086	—	978	2364	2158	2050[k]
$^{*}E_{surf}$	prism$_{(11\bar{2}0)}$	—	—	1230	—			2380	
	pyramidal$_{(1\bar{1}01)}$	—	—	1083	—	—	—	2487	
	pyramidal$_{(1\bar{1}02)}$	—	—	1225	—	—	—	2655	
$^{*}E_{sf}(I_2)$		—	—	80	—	26	62	201	340[l]
$^{*}\varepsilon(0-100\ ^{\circ}C)$		—	—	—	—	—	—	7.9	5.9[m]
$C_p(0-100\ ^{\circ}C)$		—	—	—	—	—	—	25.7	26.4[m]
Melting point		—	—	2030±160	—	—	—	1957	2128[d] (2001[d,n])
ΔH_m		—	—	—	—	—	—	16.09	21.00[d] (18.02[d,m])
$\Delta V_m/V_{solid}$		—	—	—	—	—	—	3.22	—

[a]Reference 26.
[b]Reference 32.
[c]Reference 33.
[d]Reference 34.
[e]Reference 35.
[f]Reference 37.
[g]Reference 38.
[h]Reference 39.
[i]Reference 40. (first-principles calculation)
[j]Reference 41. (first-principles calculation)
[k]Reference 42.
[l]Reference 43.
[m]Reference 45.
[n]for metastable melting of hcp Zr (calculated).

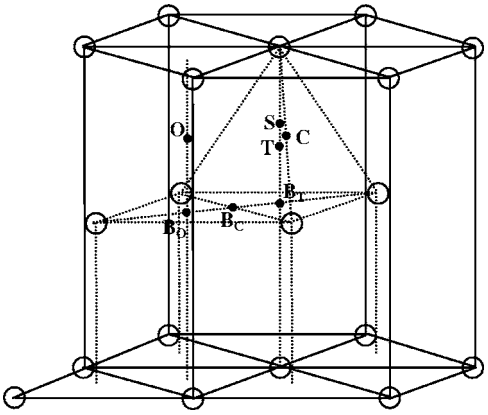

FIG. 1. Seven interstitial sites in the hexagonal closed-packed lattice.

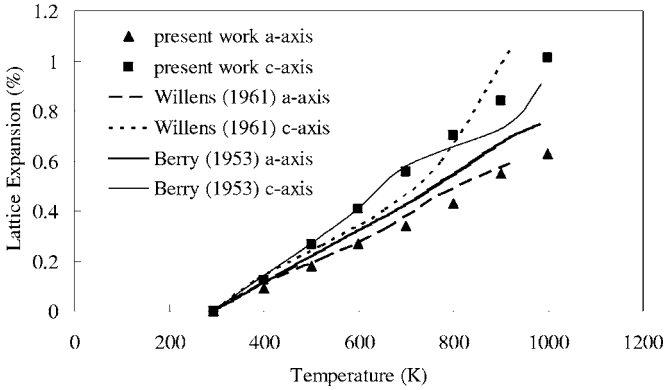

FIG. 2. Thermal linear expansion of hcp Ti in the *a* and *c* directions. Symbols are the present calculation and lines are experimental data (Refs. 47 and 48).

those used for other elements with different structures, bcc,[29] fcc,[30] and diamond,[51] which means that the potentials can be easily extended to multicomponent systems composed of wide range of elements. The MEAM potential had been successfully applied to cascade simulation of Fe-Cu alloys.[52] Therefore, it should be also possible to apply the present potential for Zr to the prediction of irradiation behavior of pure Zr and Zr-based alloys. Further, it should be mentioned here that the present potentials have been already applied to develop Cu-Ti and Cu-Zr alloy potentials to investigate the amorphous/nano-crystalline composite behavior.[53]

V. CONCLUSION

The stability problem found in the original MEAM potentials for hcp elements, Ti and Zr, has now been solved by reoptimizing the potential parameter values. Even though the more general 2NN MEAM formalism was used for the parametrization, it was eventually found that the original 1NN MEAM formalism was enough at least for Ti and Zr. The new interatomic potentials for Ti and Zr show the stability of hcp structures correctly, and describe the bulk properties (elastic constants, structural energy differences), point defect properties (vacancy, divacancy, and interstitial formation energy, activation energy of vacancy diffusion), planar defect properties (stacking faults energy, surface energy), and thermal properties (thermal expansion coefficients, specific heat, melting point, enthalpy of melting) of Ti and Zr, in good agreement with relevant experimental information. Because the mathematical formalism is exactly the same as those used for other elements with different structures, the potential can be easily extended to multicomponent systems composed of a wide range of elements.

TABLE V. Calculated physical properties of the bcc Ti and Zr at zero temperature, compared with experimental data. The units of the lattice parameter *a* and elastic constants *B*, C_{11}, C_{12}, C_{44} are Å and 10^{12} dyne/cm^2, respectively.

bcc Ti	Present calculation	Exp.	bcc Zr	Present calculation	Exp.[a]
Lattice parameter *a*	3.266	—	Lattice parameter *a*	3.580	3.574
B	1.139	—	*B*	1.011	0.970
C_{11}	1.298	—	C_{11}	1.182	1.040
C_{12}	1.060	—	C_{12}	0.926	0.930
C_{44}	0.781	—	C_{44}	0.688	0.380

[a]Reference 50.

ACKNOWLEDGMENTS

This work has been financially supported by a grant (code No. 05K1501-00412) from "*Center for Nanostructured Materials Technology*" under "*21st Century Frontier R&D Program*" of the Korean Ministry of Science and Technology and by the U.S. Department of Energy, Office of Basic Energy Sciences (M.I.B.).

APPENDIX

In the MEAM, no specific functional expression is given directly to the pair interaction $\phi(R)$. Instead, as mentioned already, the atomic energy (total energy per atom) is evaluated from the zero-temperature universal equation of state by

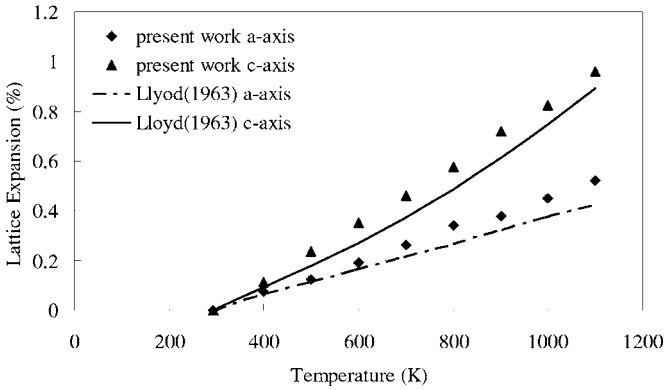

FIG. 3. Thermal linear expansion of hcp Zr in the *a* and *c* directions. Symbols are the present calculation and lines are experimental data (Ref. 49).

Rose *et al.*[16] as a function of nearest-neighbor distance R. Then, the value of $\phi(R)$ is computed from known values of the total energy and the embedding function, as a function of nearest-neighbor distance. Here, it should be noted that for a given reference structure where bonding directions among neighbor atoms are fixed, the embedding function and the energy per atom becomes a function only of the nearest-neighbor distance. If only first nearest-neighbor interactions are considered as in the original 1NN MEAM, the energy per atom can be written as follows:

$$E^a(R) = F(\bar{\rho}^o(R)) + \frac{Z_1}{2}\phi(R), \tag{A1}$$

where Z_1 is the number of nearest-neighbor atoms. The expressions for the embedding function F is available from Eq. (2). The expression for the pair interaction between two atoms separated by a distance R, $\phi(R)$, is obtained by equating the energy per atom $E^a(R)$ from Eq. (A1) to the zero-temperature universal function $E^u(R)$ from Eq. (8), as follows:

$$\phi(R) = \frac{2}{Z_1}[E^u(R) - F(\bar{\rho}^o(R))]. \tag{A2}$$

The key difference between the 1NN and 2NN MEAM is that second nearest-neighbor interactions are considered in the 2NN MEAM. In the 2NN MEAM, the summations in Eqs. (3a)–(3d) for computation of partial electron densities are extended to the second nearest-neighbor atoms. The same extension is made also in the summation for computation of pair interactions in Eq. (1). Therefore, the equation for energy per atom Eq. (A1) should be also modified so that it involves the pair interactions with second nearest-neighbor atoms as follows:

$$E^u(R) = F(\bar{\rho}^o(R)) + \frac{Z_1}{2}\phi(R) + \frac{Z_2 S}{2}\phi(aR), \tag{A3}$$

where Z_1 and Z_2 are the number of first and second nearest-neighbor atoms, respectively. S is the screening factor for second nearest neighbor interactions, and a is the ratio between the second and first nearest-neighbor distances. It should be noted that for a given reference structure S and a are constants, and the total energy and the embedding energy become functions of only nearest-neighbor distance R. Here, the computation of pair interaction is not trivial because Eq. (A3) contains two pair interaction terms. In order to derive an expression for the pair interaction, $\phi(R)$, another pair potential, $\psi(R)$, is introduced.

$$E^u(R) = F(\bar{\rho}^o(R)) + \frac{Z_1}{2}\psi(R), \tag{A4}$$

where

$$\psi(R) = \phi(R) + \frac{Z_2 S}{Z_1}\phi(aR). \tag{A5}$$

$\psi(R)$ can be computed from Eq. (A4) as a function of R, as follows:

$$\psi(R) = \frac{2}{Z_1}[E^u(R) - F(\bar{\rho}^o(R))], \tag{A6}$$

and the expression for the pair interaction $\phi(R)$ is obtained from Eq. (A5) as follows:

$$\phi(R) = \psi(R) + \sum_{n=1} (-1)^n \left(\frac{Z_2 S}{Z_1}\right)^n \psi(a^n R). \tag{A7}$$

Here, the rapidly convergent summation is performed until a specified tolerance is met for the energy of the reference structure.

*Corresponding author: B.-J. Lee, calphad@postech.ac.kr; tel: +82-54-2792157; fax: +82-54-2792399

[1] A. Akhtar, Metall. Trans. A **6A**, 1105 (1975).
[2] N. Munroe, X. Tan and H. Gu, Scr. Mater. **36**, 1383 (1997).
[3] A. Rogerson, J. Nucl. Mater. **159**, 43 (1988).
[4] V. Fidleris, R. P. Tucker and R. B. Adamson, in *An Overview of Microstructural and Experimental Factors that Affect the Irradiation Growth Behavior of Zirconium Alloys*, 7th International Conference on Zirconium in the Nuclear Industry, Strasbourg, 1985.
[5] A. Inoue, Acta Mater. **48**, 279 (2000).
[6] J. C. Lee, Y. C. Kim, J. P. Ahn, H. S. Kim, S. H. Lee and B.-J. Lee, Acta Mater. **52**, 1525 (2004).
[7] B.-J. Lee, J. C. Lee, Y. C. Kim and S. H. Lee, Met. Mater. Int. **10**, 467 (2004).
[8] M. S. Daw and M. I. Baskes, Phys. Rev. Lett. **50**, 1285 (1983); Phys. Rev. B **29**, 6443 (1984).
[9] M. W. Finnis and J. E. Sinclair, Philos. Mag. A **50**, 45 (1984).
[10] D. J. Bacon, J. Nucl. Mater. **159**, 176 (1988).
[11] D. J. Bacon, J. Nucl. Mater. **249**, 206 (1993).
[12] V. Rosato, M. Guillope and B. Legrand, Philos. Mag. A **59**, 321 (1989).
[13] D. J. Oh and R. A. Johnson, J. Mater. Res. **3**, 471 (1988).
[14] D. J. Oh and R. A. Johnson, J. Nucl. Mater. **169**, 5 (1989).
[15] R. A. Johnson, Philos. Mag. A **63**, 865 (1991).
[16] J. H. Rose, J. R. Smith, F. Guinea, and J. Ferrante, Phys. Rev. B **29**, 2963 (1984).
[17] R. Pasianot and E. J. Savino, Phys. Rev. B **45**, 12704 (1992).
[18] W. Hu, B. Zhang, B. Huang, F. Gao, and D. J. Bacon, J. Phys.: Condens. Matter **13**, 1193 (2001).
[19] M. Igarashi, K. Khantha, and V. Vitek, Philos. Mag. B **63**, 603 (1991).
[20] G. J. Ackland, Philos. Mag. A **66**, 917 (1992).
[21] G. J. Ackland, S. J. Wooding and D. J. Bacon, Philos. Mag. A **71**, 553 (1995).
[22] G. J. Ackland and V. Vitek, Phys. Rev. B **41**, 10324 (1990).
[23] F. Willaime and C. Massobrio, Phys. Rev. B **43**, 11653 (1991).
[24] F. Cleri and V. Rosato, Phys. Rev. B **48**, 22 (1993).
[25] M. I. Baskes, Phys. Rev. B **46**, 2727 (1992).
[26] M. I. Baskes and R. A. Johnson, Modell. Simul. Mater. Sci. Eng.

2, 147 (1994).
[27] K. Mae, T. Nobata, H. Ishida, S. Motoyama, and Y. Hiwatari, Modell. Simul. Mater. Sci. Eng. **10**, 205 (2002).
[28] B.-J. Lee and M. I. Baskes, Phys. Rev. B **62**, 8564 (2000).
[29] B.-J. Lee and M. I. Baskes, H. Kim, and Y. K. Cho, Phys. Rev. B **64**, 184102 (2001).
[30] B.-J. Lee, J.-H. Shim, and M. I. Baskes, Phys. Rev. B **68**, 144112 (2003).
[31] M. I. Baskes, Mater. Chem. Phys. **50**, 152 (1997).
[32] *Structure of Metals*, edited by C. S. Barrett and T. B. Massalski (McGraw-Hill, New York, 1966).
[33] *Single Crystal Elastic Constants and Calculated Aggregate Properties: A Handbook* 2nd edition, edited by G. Simmons and H. Wang (MIT Press, Cambridge, 1971).
[34] A. T. Dinsdale, CALPHAD: Comput. Coupling Phase Diagrams Thermochem. **15**, 317 (1991).
[35] *Cohesion in Metals; Transition Metal Alloys*, edited by F. R. de Boer, W. C. M. Mattens, A. R. Miedema, and A. K. Niessen (North-Holland, Amsterdam, 1988).
[36] M. Kopper, Chr. Herzig, M. Friesel and Y. Mishin, Acta Mater. **45**, 4181 (1997).
[37] H. H. Neely, Radiat. Eff. **3**, 189 (1970).
[38] G. M. Hood, R. J. Schultz, and J. A. Jackman, J. Nucl. Mater. **126**, 79 (1984); G. M. Hood and R. J. Schultz, *ibid.* **151**, 172 (1988).
[39] N. Matsuura, G. M. Hood, and H. Zou, J. Nucl. Mater. **238**, 260 (1996).
[40] F. Willaime, J. Nucl. Mater. **323**, 205 (2003).
[41] C. Domain, A. Legris, Philos. Mag. **85**, 569 (2005).
[42] W. R. Tyson and W. A. Miller, Surf. Sci. **62**, 267 (1977).
[43] P. B. Legrand, Philos. Mag. B **49**, 171 (1984).
[44] P. G. Partridge, Metall. Rev. **12**, 169 (1967).
[45] *Smithells Metals Reference Book* 7th edition, edited by E. A. Brandes and G. B. Brook (Butterworth-Heinemann, Oxford, 1992).
[46] *Thermophysical Properties of Matter*, edited by Y. S. Touloukian, R. K. Kirby, R. E. Taylor, and P. D. Desai (Plenum, New York, 1975), Vol. 12.
[47] R. H. Willens, U. S. Air Force Office of Scientific Research Report AFOSR-1839, 1961. Quoted in Ref. 46.
[48] R. L. P. Berry and G. V. Raynor, unpublished work, 1953. Quoted in Ref. 46.
[49] L. T. Lloyd, Argonne National Laboratory Report ANL-6591, 1963. Quoted in Ref. 46.
[50] A. Heiming, W. Petry, J. Trampenau, M. Alba, C. Herzig, H. R. Schober, and G. Vogl, Phys. Rev. B **43**, 10948 (1991).
[51] B.-J. Lee and J. W. Lee, CALPHAD: Comput. Coupling Phase Diagrams Thermochem. **29**, 7 (2005).
[52] B.-J. Lee, B. D. Wirth, J.-H. Shim, J. Kwon, S. C. Kwon, and J.-H. Hong, Phys. Rev. B **71**, 184205 (2005).
[53] Y.-M. Kim and B.-J. Lee, Pohang University of Science and Technology, Korea, unpublished work (2005).